Modes of Tropical Variability under Convective Adjustment and the Madden–Julian Oscillation. Part I: Analytical Theory

J. DAVID NEELIN AND JIA-YUH YU

Department of Atmospheric Sciences, University of California, Los Angeles, Los Angeles, California

(Manuscript received 26 October 1992, in final form 11 October 1993)

ABSTRACT

The interaction between the collective effects of cumulus convection and large-scale dynamics is examined using the Betts–Miller moist convective adjustment (MCA) parameterization in a linearized primitive equation model on an equatorial β plane. In Part I of this paper, an analytical approach to the eigenvalue problem is taken using perturbation expansions in the cumulus adjustment time, which is short compared to planetary dynamical time scales. The modes of tropical variability that arise under MCA are dominated by the presence of moist processes; some modes act to adjust the system rapidly toward a convectively adjusted state, while others evolve on time scales set by the large-scale dynamics subject to near-adjusted (quasi equilibrium) thermodynamical constraints. Of the latter, a single vertical mode stands out, which obeys special balances implied by the quasi-equilibrium constraints and is the only propagating deep convective mode. The propagation speed is determined by an internally defined gross moist stability. For the Kelvin meridional mode, the phase speed and vertical structure are highly suggestive of those of the Madden–Julian (MJ) oscillation.

For the simple case considered here, which assumes a homogeneous, separable basic state and sufficiently large zonal scales, the modes of variability found under MCA are all stable under reasonable conditions, although a large subclass of modes (including the MJ mode) is only slowly decaying. This contrasts with many studies using Kuo-like convective parameterizations, which have conjectured that convective instability of the second kind (CISK) plays a role in maintaining planetary-scale tropical variability. The authors suggest that a terminology is needed by which to refer to convective interaction with dynamics (CID), without necessarily assuming that large-scale instability arises from this interaction. Under MCA, there is strong CID but not generally CISK. Instability of the MJ mode can occur through evaporation–wind feedback. This behavior under MCA provides a suggestive prototype for tropical motions evolving under quasi-equilibrium convective constraints.

1. Introduction

In the Tropics, interaction between large-scale circulation and cumulus convection has long been recognized as crucial to the understanding of large-scale perturbations, and this characteristic distinguishes the dynamics of the Tropics from that of midlatitudes. Studies of the interaction between the large-scale circulation and various types of cumulus parameterization under simplifying assumptions have been used, for better or for worse, to interpret various tropical phenomena from hurricanes to the Madden–Julian Oscillation (MJO). Such models are often referred to as "CISK" (conditional instability of the second kind) models despite the fact that instability is not always found and may be unrealistic. Use of the term "CISK" dates back to Charney and Eliassen (1964) and Ooyama (1964), in an attempt to explain the formation of hurricanes by feedback between large-scale low-level convergence induced by Ekman pumping and organized cumulus convection. Subsequently, "wave–CISK" was introduced by Yamasaki (1969), Hayashi (1970), and Lindzen (1974a), in which the collective effects of convection interact directly with large-scale circulation, typically through feedbacks between latent heating and the low-level convergence induced by the resulting tropical wave motions.

Obviously, the manner in which the collective effects of cumulus convection are parameterized is key in such studies. Currently, three main types of schemes are in widespread use in large-scale general circulation models (GCMs): moist-convective adjustment schemes (Manabe et al. 1965; Betts 1986), Kuo-type schemes (Kuo 1965, 1974), and Arakawa–Schubert schemes (Arakawa and Schubert 1974). Both Kuo-like and Arakawa–Schubert-like schemes have been used in CISK models, especially the former.

Kuo-type schemes are based on closures that directly link the coupling of the latent heating and moisture sink with the supply of moisture and dry static energy by the large-scale fields, typically partitioning moisture convergence between latent heating and moistening

Corresponding author address: J. David Neelin, Department of Atmospheric Sciences, University of California, Los Angeles, Los Angeles, CA 90024-1565.
Internet: neelin@nino.atmos.ucla.edu

with a disposable parameter. For definiteness, we note that the heating is typically of the form $[(1 - b)M_t(T_c(p) - T(p))/(\hat{T}_c - \hat{T})]$ (following Kuo 1974), where M_t is the total column moisture supply by large-scale convergence and other sources, b a partition parameter, $\widehat{(\ )}$ denotes vertical averaging, and the cloud reference profile, T_c, may be from a simple cloud model. With a few exceptions (e.g., Sui and Lau 1989), CISK studies with Kuo-like schemes simplify this by fixing the vertical profile of the heating, that is, replacing $(T_c(p) - T(p))/(\hat{T}_c - \hat{T})$ by a specified function of pressure, so that latent heating is simply a function of large-scale low-level convergence (Hayashi 1970, 1971a,b,c; Lindzen 1974a,b; Chang and Piwowar 1974; Chang 1976, 1977; Stevens and Lindzen 1978; Davies 1978; Nehrkorn 1986; Chang and Lim 1988). Because there is always a degree of arbitrariness in the specification of the heating profile and magnitude relative to the low-level convergence, CISK studies with Kuo-like schemes produce instability relatively easily. In linear Kuo-like CISK, it is difficult to avoid the "ultraviolet catastrophe" in which the shortest waves are the most unstable, which fails to explain the dominance of planetary scales in tropical power spectra.

The Arakawa–Schubert (1974) scheme employs a closure assumption based on the quasi equilibrium of the cloud work function, a measure of work done by buoyancy in the cloud. Arakawa and Chen (1987) pointed out the relation between this quasi-equilibrium point of view and a generalization of convective adjustment. Stark (1976) used a linearized Arakawa–Schubert scheme in a CISK study and found that weakly unstable waves may be generated but only when the precipitation is unusually efficient. Crum and Stevens (1983) compared two different cumulus parameterization schemes in generating CISK and found that the growth rates obtained with the Arakawa–Schubert-like scheme are smaller than those obtained with a Kuo-like scheme in Stevens and Lindzen (1978).

The moist convective adjustment (MCA) scheme was first employed by Manabe et al. (1965). The basic assumption of MCA is that in convective situations the vertical temperature and moisture structures in large-scale models are strongly controlled by convection and are adjusted accordingly to reach a quasi-equilibrium state. Manabe et al. suggested "instantaneous" adjustment (in practice, at the model time step) toward a quasi-equilibrium state, which is usually chosen to be moist adiabatic, between the cloud-field and the large-scale forcing whenever the atmosphere is conditionally unstable. A number of observational studies suggest that quasi-equilibrium assumptions hold for large space and time scales (Arakawa and Schubert 1974; Lord and Arakawa 1980; Lord 1982; Arakawa and Chen 1987) and also indicate that the more restrictive quasi equilibrium of the type employed in MCA holds well over tropical ocean regions (Arakawa and Chen 1987).

Recently, Betts (1986) and Betts and Miller (1986) proposed a gentler form of convective adjustment that relaxes the atmosphere toward a selected quasi-equilibrium reference profile. The adjustment reference profile, not necessarily exactly moist adiabatic, is carefully chosen to represent thermodynamic structures typically observed in convective situations in the Tropics. The introduction of a relaxation time in the Betts–Miller scheme seems appropriate for the representation of convective adjustment processes by cumulus clouds that have finite lifetimes and makes the numerical implementation of the scheme less dependent on the model time step. Betts and Miller (1986) also indicated significant improvement of the ECMWF model forecasts under this scheme. More important for our purposes, the Betts–Miller version permits an analytical approach to examine the effects of MCA on the large-scale dynamics. As we shall see, the instantaneous adjustment case is a singular limit of this. It has been pointed out to us (A. Arakawa 1993, personal communication) that the analytical version used here is more general than the case described in Betts and Miller (1986); some numerical implementations of Betts–Miller may also differ from the smoothly posed case we treat. We will use the term "smooth MCA" where generality is required, "Betts–Miller" everywhere else.

In spite of the fact that convective adjustment schemes are used in some widely cited GCMs (e.g., GFDL and ECMWF), no CISK study has yet examined the modes that arise under convective adjustment. A version of the Betts–Miller scheme is used in a linear model on the equatorial β plane for this purpose. While nonlinearity enters the tropical circulation at many scales, such an analysis may be rigorously justified as a means of understanding the behavior of GCMs using a given convective parameterization, provided the linearization is carried out about a suitable basic state, taking the GCM as a nonlinear dynamical system to be understood by successive linearizations. However, beyond providing an analysis of the modes of variability, which arise in a primitive equation model under MCA, the results have some obvious applications to 1) the MJO, versions of which are simulated in GCMs, and 2) the question of instability through CISK.

The MJO, discovered by Madden and Julian (1971, 1972), is the strongest intraseasonal signal in the troposphere. Comprehensive descriptions of the MJO began to emerge in the early 1980s based on the observations of wind, pressure, convective activities, and outgoing longwave radiation (e.g., Lau and Chan 1983a,b; Krishnamurti et al. 1985; Lau and Chan 1985). The MJO is characterized by global-scale eastward propagation of zonal wind and convection anomalies dominated by low zonal wavenumbers. Various hypotheses concerning the mechanism maintaining the MJO include Kelvin wave–CISK, thermal forcing, lateral forcing by midlatitude disturbances, and evapora-

tion–wind feedback. Kelvin wave–CISK was first suggested by Lindzen (1974a) as a likely mechanism for the MJO and numerous papers have followed on this hypothesis (Chang 1977; Lau and Peng 1987; Chang and Lim 1988; Sui and Lau 1989). However, almost all the CISK studies have difficulty in explaining the planetary scale of the observed MJO. Recently, oscillations that resemble observations in several respects have been diagnosed in GCM simulations (Hayashi and Sumi 1986; Lau et al. 1988). These GCM studies have successfully simulated the eastward propagation of the MJO, although almost all produce propagation speeds significantly larger than those observed. The evaporation–wind feedback mechanism—in which anomalies in evaporation, created by changes in wind speed, feed back on the circulation through convection—has been shown to be important in some GCMs (Neelin et al. 1987; Numaguti and Hayashi 1991a,b), while its significance remains untested in others.

Observations of the tropical atmosphere suggest that regions experiencing deep convection are nearly neutral (Betts 1982; Xu and Emanuel 1989). Recently, Randall and Wang (1992) found that the tropical atmosphere, indeed, does not contain much moist available energy (MAE). Their results question the existence of CISK in the sense of creating instability through net release of convective available potential energy at large scales. This suggests that schemes that do not take local column stability criterion adequately into account may not properly represent the bulk effects of tropical convection, and implies that CISK studies, which use unstable thermodynamic basic states, are introducing an unrealistic energy source for large-scale disturbances. On the other hand, there are numerous tropical phenomena, such as the MJO, in which the interaction of the bulk effects of convection with the large-scale dynamics is an obvious feature. The term "CISK" is often used loosely to refer to this interaction, even though no instability may be present. A change in terminology is needed to separate these two effects; it happens that MCA, due in part to its simplicity and strong dependence on thermodynamics, provides a useful example to motivate this more general discussion.

In Part I of this paper, we formulate the model and focus on analytical results. In section 2, the vertical structure equation and horizontal structure equation are derived; the MCA convective scheme necessitates a slight variant in the setup of the eigenvalue problem relative to previous studies. The cumulus parameterization scheme employed in this study and the evaporation–wind feedback are discussed in section 3. In section 4, we briefly summarize the vertical structure equations used in the analytical work. Analytical solutions are presented at length in section 5 for the several classes of eigenmode that arise. Discussion of the implications for understanding GCMs using MCA, the dynamics of the MJO, and CISK versus CID (convective interaction with dynamics) is found in section 6.

2. Model dynamics

Since we are interested in motions that have large scales in the zonal direction, the long-wave approximation on the equatorial β plane will be employed. This approximation is not essential to the results, but the resulting simplifications give us a neatly tractable eigenvalue problem.

a. Basic equations

The momentum, continuity, hydrostatic, thermodynamic, and moisture equations in the long-wave approximation, expressed in terms of perturbations about a stratified resting basic state on the equatorial β plane ($f = \beta y$), are

$$\partial_t u' - \beta y v' + \partial_x \phi' = -\epsilon_m u' + \mathcal{N}_u, \tag{2.1a}$$

$$\beta y u' + \partial_y \phi' = \mathcal{N}_v, \tag{2.1b}$$

$$\partial_x u' + \partial_y v' + \partial_p \omega' = 0, \tag{2.1c}$$

$$\partial_p \phi' = -(R/p)T', \tag{2.1d}$$

$$\partial_t T' + C_p^{-1}(\partial_p \bar{S})\omega' = Q_c'(T', q', T_b', q_b', \bar{T}) - \epsilon_r T' + \mathcal{N}_T, \tag{2.1e}$$

$$\partial_t q' + (\partial_p \bar{q})\omega' = Q_q'(T', q', \bar{T}) + \mathcal{N}_q, \tag{2.1f}$$

$$\partial_t T_b' + C_p^{-1}(\Delta \bar{S}_b/\Delta p_b)\omega_b' = Q_c'(T', q', T_b', q_b', \bar{T}) - \epsilon_b T_b' + \mathcal{N}_{T_b}, \tag{2.1g}$$

$$\partial_t q_b' + (\Delta \bar{q}_b/\Delta p_b)\omega_b' = Q_q'(T_b', q_b', \bar{T}) + E'(\Delta p_b/g)^{-1} + \mathcal{N}_{q_b}. \tag{2.1h}$$

The notation used here is conventional with u', v', ϕ', T', ω', and q' denoting zonal velocity, meridional velocity, geopotential height, temperature, pressure velocity, and specific humidity, respectively. Subscript b denotes boundary-layer variables. A simple Rayleigh friction, with decay rate ϵ_m, appears in the u-momentum equation; it may be viewed as crudely standing in for other forms of mechanical damping, or possibly as roughly representing a cumulus friction effect. A Newtonian cooling term, with decay rate ϵ_r, applies in the thermodynamic equation representing the radiative cooling effect; while ϵ_b is used in the boundary layer to denote PBL temperature damping rate. Here R is the gas constant and S is the dry-static energy defined as $(C_pT + \phi)$, where C_p is the specific heat at constant pressure; E' denotes surface evaporation (in units of kg m^{-2} s^{-1}), which only applies in the boundary-layer moisture equation; $\Delta \bar{S}_b$ and $\Delta \bar{q}_b$ denote, respectively, the jumps of dry static energy and specific humidity between boundary layer and the troposphere; and Δp_b is the pressure depth of the boundary layer. In the above

equations, all dependent variables are perturbations with respect to a basic state, denoted $\overline{(\ )}$. The convective heating, Q_c', and moisture source, Q_q', are functions of perturbation and the basic-state thermodynamic quantities, T', q', T_b', q_b', $\bar{T}$, as will be specified in the cumulus parameterization discussed in section 3. The nonlinear terms, $\mathcal{N}_u$, $\mathcal{N}_v$, $\mathcal{N}_T$, $\mathcal{N}_q$, $\mathcal{N}_{T_b}$, $\mathcal{N}_{q_b}$, are of second order and higher in the perturbation variables and are negligible for sufficiently small perturbations. We write them for reference in discussing the relation of linear to nonlinear behavior of the system. The nonlinear terms will all have a contribution from advection, that is, from terms $\mathbf{v}' \cdot \nabla(u', v', T', \ldots)$. Under suitable spatial discretization, these advective nonlinearities will all be smooth functions of the perturbation quantities. There will also be a contribution to the nonlinear terms $\mathcal{N}_T$, $\mathcal{N}_q$, $\mathcal{N}_{T_b}$, $\mathcal{N}_{q_b}$ from the cumulus parameterization, as discussed below.

In deriving (2.1e) and (2.1f), we have assumed a spatially uniform basic state such as might occur in a very idealized version of a GCM with uniform sea surface temperature lower boundary conditions or, more realistically, with zonally symmetric boundary conditions whose y variations were slow, say order δ_y, compared with the equatorial radius of deformation and neglecting terms of $O(\delta_y)$. Under MCA, this will lead to a self-consistent steady state in radiative–convective equilibrium (RCE), with latent heating balancing radiative cooling and moisture source balancing evaporation as well as total latent heating balancing total moisture sink at each point and negligible baroclinic circulation in the basic state. The basic-state balances are just

$$\bar{Q}_c + \bar{Q}_R = 0, \tag{2.2a}$$

$$\bar{Q}_q + \bar{E}(\Delta p_b/g)^{-1} = 0, \tag{2.2b}$$

$$C_p \int_{p_T}^{p_0} \bar{Q}_c \frac{dp}{g} = -L \int_{p_T}^{p_0} \bar{Q}_q \frac{dp}{g} = L\bar{E}. \tag{2.2c}$$

For the cumulus parameterization considered here, there is a finite neighborhood about the RCE stationary point for which the contributions of the heating and moisture sink to the nonlinear terms $\mathcal{N}_T$, $\mathcal{N}_q$, $\mathcal{N}_{T_b}$, $\mathcal{N}_{q_b}$ are also smooth functions of the prognostic variables. We thus have a case in which the system satisfies the conditions of the center manifold theorem (e.g., Guckenheimer and Holmes 1983), implying that certain qualitative aspects of the nonlinear behavior in some neighborhood of the radiative equilibrium state can be deduced from the linear eigenvalue problem about that state. In drawing conclusions from the analytical analysis of the linear problem, we will have a set of specific conditions where statements can be made rigorously, although of course there will also be areas where the linear analysis can only be suggestive.

b. Separation of variables

Linearizing (2.1) and decomposing all perturbation variables, including Q_c', Q_q', and E', as

$$(\ )'(x, y, p, t) = \tilde{(\ )}(y, p)e^{\lambda t}e^{ikx}, \tag{2.3}$$

where k is zonal wavenumber and λ is a complex eigenvalue, the momentum equations, continuity equation, and hydrostatic equation, (2.1a)–(2.1d), give

$$\frac{p}{R}\beta^2 y^3 \partial_p^2 \tilde{\omega} + (\lambda + \epsilon_m) y \partial_y^2 \tilde{T} - 2(\lambda + \epsilon_m)\partial_y \tilde{T} + ik\beta y \tilde{T} = 0, \tag{2.4}$$

which with the thermodynamic and moisture equations and the cumulus parameterization yields a two-dimensional (y, p) eigenvalue problem.

For the separable case considered here, if ϵ_r, ϵ_m, $\partial_p \bar{S}$, and $\partial_q \bar{q}$ are all independent of y, we can consistently assume that all thermodynamic variables and ω are separable with the same y structure:

$$\tilde{(\ )}(y, p) = (\ )(p)Y(y), \tag{2.5}$$

where $Y(y)$ is the y-structure function. Equation (2.4) thus can be separated into vertical and horizontal structure equations, provided ϵ_m is independent of p, which gives

$$\partial_p^2 \omega - r\frac{R}{p}T = 0, \tag{2.6}$$

and

$$(\lambda + \epsilon_m) y \partial_y^2 Y - 2(\lambda + \epsilon_m)\partial_y Y + r\beta^2 y^3 Y(y) + ik\beta y Y = 0, \tag{2.7}$$

where r is a constant of separation. Comparing (2.7) to the corresponding horizontal structure equation for the shallow-water equations, it is convenient to define $c^2 \equiv -(\lambda + \epsilon_m)/r$ where c^2 is now the separation constant, proportional to equivalent depth. This leads to the familiar nondimensionalization with inverse length scale, $\mu = (\beta/c)^{1/2}$ and time scale $(\mu c)^{-1}$. Defining $y^* = \mu y$, $k^* = k/\mu$ and $\lambda^* = (\mu c)^{-1}\lambda$, the nondimensional form of (2.7) is

$$y^* \partial_{y^*}^2 Y - 2\partial_{y^*} Y - y^{*3} Y + \frac{ik^*}{\lambda^* + \epsilon_m^*} y^* Y = 0. \tag{2.8}$$

Since this is the same horizontal structure equation as for the shallow-water equations on a β plane with the long-wave approximation, the solutions must satisfy the condition:

$$\lambda_n^* + \epsilon_m^* = \frac{ik^*}{(2n + 1)}, \tag{2.9}$$

and

$$Y(y^*) = \frac{i(\lambda_n^* + \epsilon_m^*)}{k^*}\left(-\frac{d\psi_n(y^*)}{dy^*}\right) + y^*\psi_n(y^*), \tag{2.10}$$

that is, for given n,

$$Y(y^*) = \frac{1}{2}\left[1 - \frac{1}{(2n+1)}\right]\psi_{n+1}(y^*) + \left[\frac{n}{(2n+1)} + n\right]\psi_{n-1}(y^*), \quad (2.11)$$

where the Hermite function, $\psi_n(y^*)$, is defined as $\psi_n(y^*) = \exp(-y^{*2}/2)H_n(y^*)$ and $H_n(y^*)$ is the nth-order Hermite polynomial. The dimensional form of (2.9) is

$$\lambda_n + \epsilon_m = \frac{ik}{(2n+1)}c. \quad (2.12)$$

The case $n = 0$ corresponds to the anti-Kelvin wave, which is eliminated by y boundary conditions. The case $n = -1$ is the Kelvin wave, $n = 1$ is the gravest Rossby wave with phase speed one-third of the Kelvin wave phase speed, and the higher meridional Rossby modes ($n = 2, 3, \cdots$) are correspondingly slower. Modes that have pure real eigenvalues ($\lambda_n + \epsilon_m$) effectively have negative equivalent depth in the horizontal structure equation but are thermodynamically direct in the vertical structure equation. Having used the horizontal structure equation to get the relationship (2.12) between the time eigenvalue and the separation constant, employing the definition of c and (2.6) gives the combined contribution of momentum, continuity, and hydrostatic equations to the vertical structure equations:

$$(\lambda_n + \epsilon_m)\partial_p^2\omega - \frac{R}{p}\frac{k^2}{(2n+1)^2}T = 0. \quad (2.13)$$

In this form, (2.13) will always produce a spurious set of roots with phase speed of the wrong sign, but these are easily eliminated by reference to the y boundary conditions, giving the eastward Kelvin wave and westward long Rossby waves in the propagating case. The vertical structure equation of the Kelvin mode ($n = -1$) is identical to nonrotating gravity wave equations, as far as eigenvalue is concerned, and will hold for all wavenumbers. For Rossby modes ($n = 1, 2, 3, \cdots$), the long-wave approximation only holds for

$$k \ll |\mu| = \left|\frac{\beta k}{(2n+1)(\lambda_n + \epsilon_m)}\right|^{1/2}, \quad (2.14)$$

that is, for

$$k \ll \frac{\beta}{(2n+1)|\lambda_n + \epsilon_m|}. \quad (2.14')$$

For modes with small $|\lambda_n + \epsilon_m|$, the approximation for Rossby waves can hold to large wavenumbers. The dispersion diagram and eigenmode vertical structures as a function of k are identical for the Kelvin wave and long Rossby waves except that k^2 is modified by a factor of $(2n+1)^{-2}$ for the Rossby mode case. This is convenient since we need only to display solutions for the Kelvin case, and the Rossby case follows immediately. However, the primary reason for making use of the long-wave approximation is the simplicity of the solutions to the horizontal structure equation, which yields (2.13) and thus a simple eigenvalue problem of standard form. Without the long-wave approximation, the dependence of the latent heating and moistening upon thermodynamic variables in MCA leads to a more difficult eigenvalue problem. We note that the form considered here is equally valid for nonrotating gravity waves, and so may be used to examine the limit of small scales, as well as for long zonal scales. For the Kelvin wave, it holds uniformly for all scales.

3. Model physics

a. *Parameterization of cumulus convection*

According to the Betts (1986) parameterization for cumulus convection, the latent heating and moisture source are represented as

$$Q_c' = \frac{1}{\tau_c}(T_c' - T' - \Delta T_c'), \quad (3.1a)$$

$$Q_q' = \frac{1}{\tau_c}(q_c' - q'), \quad (3.1b)$$

where T_c' and q_c' are, respectively, the temperature and specific humidity reference profiles toward which convective adjustment occurs, which are themselves functions of the basic state and large-scale thermodynamic variables. Here $\Delta T_c'$ is the energy correction, which satisfies the enthalpy constraint. All quantities in (3.1) are written in terms of perturbations from the RCE state; the form remains smooth and linearizable provided the convective adjustment is operating, that is, for a finite range of perturbation amplitude (which depends on the basic state).

The relaxation time scale of cumulus convection, τ_c, is introduced to simulate the characteristic time over which convective motions tend to bring the changing large-scale field toward a quasi-equilibrium reference state. With small τ_c the model atmosphere adjusts rapidly toward the specified thermodynamic profile, while with large τ_c the thermodynamics is less tightly constrained. Betts (1986) suggested that an appropriate value of τ_c is about two hours, with τ_c being chosen to approximate $\Delta\tilde{p}/\omega_{\max}$, where $\Delta\tilde{p}$ is the pressure depth required to lift the air parcel before it is saturated and $\omega_{\max}$ is the maximum pressure velocity in convection.

The scheme also employs an energy constraint, which requires that the total heating must balance the total moisture sink:

$$C_p\int_{p_T}^{p_0} Q_c'\frac{dp}{g} = -L\int_{p_T}^{p_0} Q_q'\frac{dp}{g}, \quad (3.2)$$

where p_T and p_0 denote the pressure level at cloud top

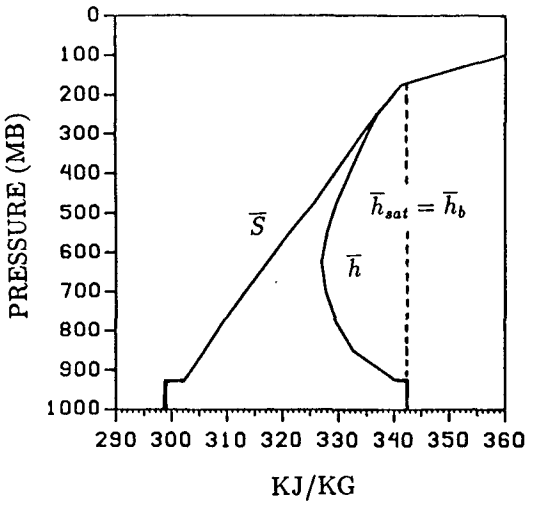

FIG. 1. Profiles of basic-state dry static energy $\bar{S}$ and basic-state moist static energy $\bar{h}$ [following Jordan (1958), except that the lowest 75 mb is approximated by a well-mixed boundary layer].

and sea surface level, respectively. This closure assumption (3.2) links the moisture equation with the temperature equation and will give a correction term to the latent heating reference profile as outlined below.

1) REFERENCE PROFILE OF SPECIFIC HUMIDITY

For the reference profile of the specific humidity, we let q_c be a given fraction of saturation; that is,

$$q'_c = \alpha q'_{\rm sat}(\bar{T}), \tag{3.3}$$

where $\alpha(p)$ is a measure of relative humidity and $Lq'_{\rm sat}(\bar{T}) = \gamma C_p T'$. Here γ is a unitless variable defined as $\gamma = d(Lq_{\rm sat})/d(C_pT)|_{\bar{T}}$ and $q_{\rm sat}(\bar{T})$ is the saturation specific humidity. When $\alpha = 1$, the reference atmosphere is saturated; from many observational studies, α ranges from 0.8 to 0.9 for most tropical precipitation systems. Betts (1986) specifies α as a function of p and $\bar{T}$, with a minimum at the freezing level (note that there is a simple one-to-one correspondence between α and the $\mathcal{P}^*$ parameter used by Betts). In analytical work, we either leave α as a general function of p or treat it as a constant.

2) REFERENCE PROFILE OF TEMPERATURE

The Betts (1986) specification for the deep convective reference temperature profile is chosen to represent observed structure and is not necessarily moist adiabatic. However, it is relatively close to the moist adiabat arising from the boundary layer, and we use this as our standard reference profile for numerical work, consistent with classic Manabe convective adjustment. In analytical work, we either leave the reference profile in general form or make further simplifications. We are concerned here only with perturbations to the reference profile. The perturbation reference temperature, T'_c, obeys

$$h'_{\rm sat}(\bar{T}, T'_c) = h'_b(T'_b, q'_b), \tag{3.4}$$

where $h'_{\rm sat}$ and h'_b are defined as:

$$h'_{\rm sat} = C_pT'_c + \phi'_c + Lq'_{\rm sat}(\bar{T}, T'_c), \tag{3.5a}$$

$$h'_b = C_pT'_b + Lq'_b. \tag{3.5b}$$

Here h'_b is defined at a reference level, p_0, at the bottom of the PBL (i.e., h'_b is both the moist enthalpy of the PBL and the moist static energy at the reference level) and $h'_{\rm sat}$ is the saturation moist static energy above the boundary layer.

Solving (3.4) yields

$$C_pT'_c(p) = A(p)h'_b \tag{3.6}$$

for all levels between cloud base (at the top of the boundary layer) and cloud top, where $\bar{h}_{\rm sat} = \bar{h}_b$. The profile $A(p)$ is just the vertical dependence of the perturbations to the temperature reference profile T'_c for a given h'_b. A derivation for this in finite-difference form is given in Part II. Figure 1 shows typical basic-state thermodynamic profiles from Jordan (1958) used to represent the observed mean tropical troposphere. For this observed basic-state temperature profile, $A(p)/p$ is given in Fig. 2. Also shown in Fig. 2 are two linear approximations to $A(p)/p$ used in sensitivity tests.

Betts (1986) suggested that for deep convection, the reference profile should be constructed to satisfy the total energy constraint (3.2), which because of the form of the heating, can be expressed as a total enthalpy constraint:

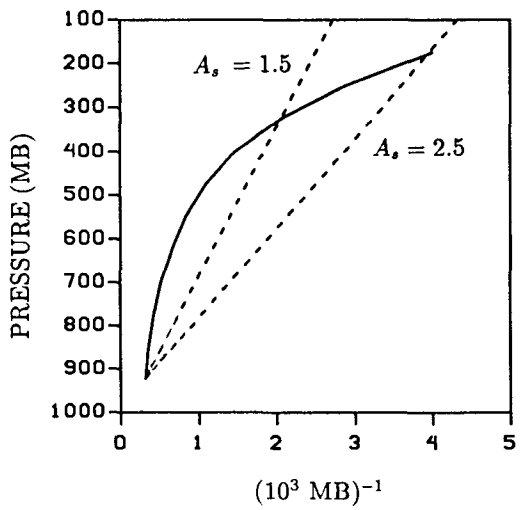

FIG. 2. $A(p)/p$, the vertical structure of the perturbation to the moist adiabat for a given perturbation of boundary-layer temperature, scaled by a compressibility-related factor, as calculated from observed basic-state thermodynamic profiles (solid line). Dashed lines show two linear approximations to $A(p)/p$ with different slopes chosen to give an estimate of sensitivity.

$$\int_{p_T}^{p_b} (H_c' - H')dp = 0, \tag{3.7}$$

where enthalpy quantities are defined as

$$H' = C_pT' + Lq', \tag{3.8a}$$

$$H_c' = C_p(T_c' - \Delta T_c') + Lq_c', \tag{3.8b}$$

with H_c denoting the corrected reference profile of enthalpy and $(T_c' - \Delta T_c')$ denoting the corrected reference profile of temperature. When (3.8a) and (3.8b) are substituted in (3.7), this is equivalent to (3.2). Thus, the total enthalpy constraint simply implies that the source of latent heating release in the cumulus convection is from the moisture sink in the troposphere.

We note that T_c' is the uncorrected reference profile defined by (3.6) and $\Delta T_c'$ is a constant correction to this profile that introduces the degree of freedom necessary to satisfy the conservation constraint (3.7). Betts and Miller (1986) solved this numerically, constructing T_c' as a first-guess reference profile, then iterating with the correction term to satisfy (3.7). Here we employ an explicit solution for the correction:

$$C_p\Delta T_c' = \Delta p_T^{-1}\left[\int_{p_T}^{p_b} C_p(T_c' - T')dp + \int_{p_T}^{p_b} L(q_c' - q')dp\right] = \hat{A}h_b' - C_p(\hat{T}' - \widehat{\alpha\gamma T'}) - L\hat{q}', \tag{3.9}$$

where Δp_T is defined as the total length of column over which convective heating applies. Here we have used $\hat{(\ )} = \Delta p_T^{-1}\int_{p_T}^{p_b}(\ )dp$ for vertically averaged quantities.

b. Evaporation–wind feedback

Neelin et al. (1987) and Emanuel (1987) jointly suggested the importance of evaporation–wind feedback in maintaining and intensifying the Madden–Julian Oscillation. A region of anomaly latent heating on the equator will force anomalous easterlies to the east of the heating region and westerlies to the west at lower levels. Since the evaporation depends on wind speed, the anomaly winds, in turn, strengthen the evaporation anomaly to the east of the heating and weaken the evaporation anomaly to the west. The resulting anomalous evaporation will then feed back, through convection, to the heating anomaly. Under proper circumstances, the evaporation–wind feedback favors eastward propagating waves. More recently, Numaguti and Hayashi (1991a,b) used an "aqua planet" GCM to study planetary-scale structures and cumulus activity. They found the existence of the MJO under two different cumulus parameterization schemes (Kuo-type and Manabe's MCA) and also concluded that the MJO is maintained by the evaporation–wind feedback mechanism. Goswami and Goswami (1991) showed strong effects of the evaporation–wind feedback on the mixed Rossby–gravity mode.

To study the impact of evaporation–wind feedback, we parameterize the evaporation term as

$$E = \rho C_D W[(\bar{q}_{\text{sat}}(T_s) + q'_{\text{sat}}(T_s)) - (\bar{q}_b + q_b')], \tag{3.10}$$

where ρ is the density of the air, C_D is the drag coefficient, T_s is the sea surface temperature, and W is the wind speed, which depends on u_b. Linearizing (3.10), we get

$$E' = (dW/du_b)\rho C_D(\bar{q}_{\text{sat}}(T_s) - \bar{q}_b)u_b' - \rho C_D\bar{W}q_b' + \rho C_D\bar{W}\gamma_s(C_p/L)T_s'. \tag{3.11}$$

Thus the evaporation term in (2.1h) can be expressed as

$$E'(\Delta p_b/g)^{-1} = -F(\Delta p_b/g)^{-1}u_b' - \epsilon_q q_b' + \epsilon_q\gamma_s(C_p/L)T_s', \tag{3.12}$$

where we have defined

$$F = -(dW/du_b)\rho C_D(\bar{q}_{\text{sat}}(T_s) - \bar{q}_b), \tag{3.13a}$$

$$\epsilon_q = \rho C_D\bar{W}(\Delta p_b/g)^{-1}. \tag{3.13b}$$

Here F is the evaporation–wind feedback parameter; F has been chosen such that it is positive when the mean zonal wind is easterly ($\bar{u}_b < 0$), noting that for the simplest parameterization, $W = |\bar{u}_b + u_b'|$, one has $(dW/du_b) = \text{sgn}(\bar{u}_b)$. The first and second terms on the right-hand side of (3.12) are the evaporation–wind feedback and the effective evaporative damping, respectively. The last term is due to sea surface temperature anomalies that are neglected in this study for the purpose of simplicity (i.e., $T_s' = 0$). Estimates from a GCM study (Neelin et al. 1987) suggest that F is in the range of 0.2 to 0.6 mm day^{-1} (m s^{-1})$^{-1}$. Estimates of the boundary-layer parameters suggest $\epsilon_q = (2 \text{ days})^{-1}$. For the Kelvin case, u has the same y structure as ω, T and q, so (3.12) is consistent with (2.5) for $n = -1$. For Rossby modes, an expansion of u in ψ_n should be employed when adding the evaporation–wind feedback.

4. Eigensystem

The cumulus convection and evaporation parameterizations formulated in section 3 close the eigenvalue problem. For convenience, the complete system determining eigenvalues and vertical structures is summarized here. For definiteness, we give the Kelvin wave meridional structure ($n = -1$) case, since the long Rossby wave or short gravity wave cases can be obtained by suitably redefining k. The combined momentum–continuity–hydrostatic equation can be expressed as

$$(\lambda + \epsilon_m)\partial_p^2\omega - k^2(\kappa/p)T = 0, \tag{4.1}$$

with thermodynamic and moisture equations for the troposphere and boundary layer:

$$(\lambda + \epsilon_r)T + (\partial_p \bar{S})\omega = \tau_c^{-1}(T_c - T - \Delta T_c), \quad (4.2a)$$

$$(\lambda + \epsilon_b)T_b + (\Delta \bar{S}_b/\Delta p_b)\omega_b = -\tau_c^{-1}\Delta T_c, \quad (4.2b)$$

$$\lambda q + (\partial_p \bar{q})\omega = \tau_c^{-1}(\alpha\gamma T - q), \quad (4.2c)$$

$$(\lambda + \epsilon_q)q_b + (\Delta \bar{q}_b/\Delta p_b)\omega_b = \tau_c^{-1}(\alpha_b\gamma_b T_b - q_b) - LF(\Delta p_b/g)^{-1}u_b, \quad (4.2d)$$

where the reference temperature is $T_c = A(p)h_b$ and the energy constraint requires

$$\Delta T_c = \hat{A}h_b - (\widehat{\hat{T} - \alpha\gamma T}) - \hat{q}, \quad (4.3)$$

although sometimes it is easier to work directly with the original version:

$$\widehat{Q_c} + \widehat{Q_q} = 0. \quad (4.3')$$

In (4.1), we have defined $\kappa = R/C_p$. For brevity, we have dropped primes and absorbed C_p and L into temperature and specific humidity so they both have energy units (J kg^{-1}).

5. Eigenmodes of the tropical atmosphere under MCA

In order to isolate the convective interaction with dynamics, the evaporation–wind feedback is temporarily neglected, but we retain the effective evaporative damping and boundary-layer temperature damping processes. The impact of the evaporation–wind feedback will be discussed separately in section 5d, with respect to the Madden–Julian mode.

By taking the convective time scale, τ_c, as a small parameter, we can decompose the system into a series of relatively simpler ones, with the first few order balances representing most of the important features. We express all variables in the form of perturbation series:

$$(\omega, T, q, \omega_b, T_b, q_b) = (\ )^{(0)} + \tau_c(\ )^{(1)} + \tau_c^2(\ )^{(2)} + \cdots$$

and eigenvalue, λ, as

$$\lambda = \tau_c^{-1}\lambda^{(-1)} + \lambda^{(0)} + \tau_c\lambda^{(1)} + \tau_c^2\lambda^{(2)} + \cdots,$$

where λ is treated differently since we expect the existence of eigenvalues of order τ_c^{-1}. These modes are termed "fast modes" since their dynamics change rapidly with the time scale of τ_c, while the others are termed "slow modes." We examine all modes for completeness, but readers interested only in the single most important mode may skip directly to section 5c.

a. Fast modes

Supposing that $\lambda^{(-1)} \neq 0$, we seek fast mode solutions. At order τ_c^{-1}, the balances are

$$\lambda^{(-1)}T^{(0)} = T_c^{(0)} - T^{(0)} - \Delta T_c^{(0)}, \quad (5.1a)$$

$$\lambda^{(-1)}T_b^{(0)} = -\Delta T_c^{(0)}, \quad (5.1b)$$

$$\lambda^{(-1)}q^{(0)} = \alpha\gamma T^{(0)} - q^{(0)}, \quad (5.1c)$$

$$\lambda^{(-1)}q_b^{(0)} = \alpha_b\gamma_b T_b^{(0)} - q_b^{(0)}, \quad (5.1d)$$

$$T_c^{(0)} = A(p)(T_b^{(0)} + q_b^{(0)}), \quad (5.1e)$$

and the energy constraint is

$$\lambda^{(-1)}\left(\int_{p_T}^{p_b} T^{(0)}dp + \int_{p_T}^{p_b} q^{(0)}dp + \Delta p_b T_b^{(0)} + \Delta p_b q_b^{(0)}\right) = 0. \quad (5.1f)$$

Here we have used the lhs of (5.1a)–(5.1d) to replace the latent heating and moisture sink in (4.3′). At $O(\tau_c^{-1})$ balance, the momentum equation does not appear and only thermodynamic variables are constrained. Note that we work in terms of T_b and q_b for these modes, rather than h_b, because the latter does not yield simplifications without convective quasi equilibrium.

From the energy constraint (5.1f), there is a possible root of $\lambda^{(-1)} = 0$ with convectively adjusted balances in (5.1a–d), which gives the slow mode solutions discussed in section 5b. The fast mode energy constraint gives

$$\widehat{T^{(0)}} + \widehat{q^{(0)}} + \frac{\Delta p_b}{\Delta p_T}T_b^{(0)} + \frac{\Delta p_b}{\Delta p_T}q_b^{(0)} = 0, \quad (5.2)$$

where $\hat{(\ )}$ denotes the vertical pressure average as in section 3. From (5.1a), (5.1b), (5.1c), and (5.1e), we obtain

$$\widehat{T^{(0)}} = \frac{\hat{A}(T_b^{(0)} + q_b^{(0)}) + \lambda^{(-1)}T_b^{(0)}}{(\lambda^{(-1)} + 1)}, \quad (5.3a)$$

$$\widehat{q^{(0)}} = \frac{\widehat{\alpha\gamma A}(T_b^{(0)} + q_b^{(0)}) + \lambda^{(-1)}\widehat{\alpha\gamma}T_b^{(0)}}{(\lambda^{(-1)} + 1)^2}. \quad (5.3b)$$

The energy constraint (5.2) thus becomes

$$\left[\left(1 + \frac{\Delta p_b}{\Delta p_T}\right)\lambda^{(-1)^2} + \left(\hat{A} + \widehat{\alpha\gamma} + 2\frac{\Delta p_b}{\Delta p_T} + 1\right)\lambda^{(-1)} + \left(\hat{A} + \widehat{\alpha\gamma A} + \frac{\Delta p_b}{\Delta p_T}\right)\right]T_b^{(0)} + \left[\frac{\Delta p_b}{\Delta p_T}\lambda^{(-1)^2} + \left(\hat{A} + 2\frac{\Delta p_b}{\Delta p_T}\right)\lambda^{(-1)} + \left(\hat{A} + \widehat{\alpha\gamma A} + \frac{\Delta p_b}{\Delta p_T}\right)\right]q_b^{(0)} = 0, \quad (5.4a)$$

which, along with the order τ_c^{-1} boundary-layer moisture equation,

$$\alpha_b\gamma_b T_b^{(0)} - (1 + \lambda^{(-1)})q_b^{(0)} = 0, \quad (5.4b)$$

provide a complete set of equations for fast mode eigenvalues to $O(\tau_c^{-1})$.

First, motivated by special balances of the free tropospheric temperature equation (5.1a), free tropospheric moisture equation (5.1c), and boundary-layer moisture equation (5.1d), we focus on the case of $\lambda^{(-1)} = -1$. This implies:

$$T_b^{(0)} = q_b^{(0)} = 0, \quad (5.5a)$$

$$T_c^{(0)} = \Delta T_c^{(0)} = q_c^{(0)} = 0, \quad (5.5b)$$

$$T^{(0)} = \widehat{q^{(0)}} = 0. \quad (5.5c)$$

Thus, these modes, with decay rate τ_c^{-1}, have zero temperature and relative humidity reference profiles and zero temperature in the troposphere. The thermodynamic variables are not perturbed in the boundary layer, and they must have wiggly specific humidity structures in the heating region to satisfy (5.5c). These eigenstructures and the order-zero eigenvalues, which provide a countable infinity of fast modes, must be solved from the next-order balances in a manner qualitatively similar to that carried out for kinematically dominated slow modes in appendix A. We omit this analysis and discuss these modes in the numerical results of Part II.

Next, we focus on the case of $\lambda^{(-1)} \neq -1$. This requires the determinant of (5.4a) and (5.4b) to vanish, which yields

$$\left(1 + \frac{\Delta p_b}{\Delta p_T}\right)\lambda^{(-1)^3} + \left(\alpha_b\gamma_b\frac{\Delta p_b}{\Delta p_T} + \hat{A} + 2 + \widehat{\alpha\gamma} + 3\frac{\Delta p_b}{\Delta p_T}\right)\lambda^{(-1)^2}$$

$$+ \left(\alpha_b\gamma_b\hat{A} + 2\alpha_b\gamma_b\frac{\Delta p_b}{\Delta p_T} + 2\hat{A} + 1 + \widehat{\alpha\gamma A} + \widehat{\alpha\gamma} + 3\frac{\Delta p_b}{\Delta p_T}\right)\lambda^{(-1)}$$

$$+ (1 + \alpha_b\gamma_b)\left(\hat{A} + \widehat{\alpha\gamma A} + \frac{\Delta p_b}{\Delta p_T}\right) = 0. \quad (5.6)$$

Solving this cubic equation numerically, for the standard basic-state parameters with $\Delta p_b = 75$ mb and $\Delta p_T = 825$ mb, yields one pure real root with $\lambda^{(-1)} = -1.58$ and a complex conjugate pair with $\lambda^{(-1)} = -0.95 \pm 0.589i$. For $\tau_c = 2$ h, the first root gives decay rate of about $(1.26\text{ h})^{-1}$; the complex pair gives decay rate of about $(2.11\text{ h})^{-1}$ and period of about 21 h. This pair appears numerically undesirable, although it is not known whether it creates difficulties in practice.

The energy balance of fast modes is between time rate change of temperature and diabatic heating, consistent with the rapid decay at rates too fast to allow the dynamics to adjust. The 0th-order thermodynamic variables are not in adjustment with the reference profiles; rather, these are the modes that would effectuate the adjustment toward quasi equilibrium from nonadjusted initial conditions (or stochastically perturbed conditions). Since these eigenmodes are degenerate at leading order, they do not individually have any physical significance in the dynamical system. Their collective effect is to maintain adjustment and the rapid decay time indicates that the degree of nonadjustment will be small.

b. Slow modes

Choosing $\lambda^{(-1)} = 0$, we now seek slow mode solutions. At order τ_c^{-1} balance, the eigen-system gives the structures of the zeroth-order thermodynamic variables:

$$T^{(0)} = T_c^{(0)}, \quad \Delta T_c^{(0)} = 0, \quad (5.7a)$$

$$q^{(0)} = q_c^{(0)} = \alpha\gamma T^{(0)}, \quad (5.7b)$$

$$q_b^{(0)} = q_c^{(0)} = \alpha_b\gamma_b T_b^{(0)}, \quad (5.7c)$$

$$T_c^{(0)} = A(p)h_b^{(0)}. \quad (5.7d)$$

For slow modes, the zeroth-order temperature and moisture profiles are exactly the same as the reference profiles and the temperature correction term is zero. Thus, there are neither latent heating nor moisture sink for order τ_c^{-1} thermodynamic balances, and the energy constraint is automatically satisfied. Only the zeroth-order thermodynamic variables are constrained at $O(\tau_c^{-1})$, leaving $\lambda^{(0)}$ and $\omega^{(0)}$ free. Physically, because the dynamical time scales of slow modes are long compared to the cumulus time scale τ_c, near adjustment to the reference profile is expected.

The zeroth-order balances yield a more complete system:

$$(\lambda^{(0)} + \epsilon_m)\partial_p^2\omega^{(0)} - k^2(\kappa/p)T^{(0)} = 0, \quad (5.8a)$$

$$(\lambda^{(0)} + \epsilon_r)T^{(0)} + (\partial_p\bar{S})\omega^{(0)} = (T_c^{(1)} - T^{(1)} - \Delta T_c^{(1)}), \quad (5.8b)$$

$$(\lambda^{(0)} + \epsilon_b)T_b^{(0)} + (\Delta\bar{S}_b/\Delta p_b)\omega_b^{(0)} = -\Delta T_c^{(1)}, \quad (5.8c)$$

$$\lambda^{(0)}q^{(0)} + (\partial_p\bar{q})\omega^{(0)} = (\alpha\gamma T^{(1)} - q^{(1)}), \quad (5.8d)$$

$$(\lambda^{(0)} + \epsilon_q)q_b^{(0)} + (\Delta\bar{q}_b/\Delta p_b)\omega_b^{(0)} = (\alpha_b\gamma_b T_b^{(1)} - q_b^{(1)}), \quad (5.8e)$$

$$T_c^{(1)} = A(p)h_b^{(1)}, \quad (5.8f)$$

with energy constraint,

$$\int_{p_T}^{p_b}[(\lambda^{(0)} + \epsilon_r)A(p)h_b^{(0)} + (\partial_p\bar{S})\omega^{(0)}]dp + \int_{p_T}^{p_b}[\lambda^{(0)}\alpha(p)\gamma(p)A(p)h_b^{(0)} + (\partial_p\bar{q})\omega^{(0)}]dp + [\Delta p_b(\lambda^{(0)} + \epsilon_b)T_b^{(0)} + \Delta\bar{S}_b\omega_b^{(0)}] + [\Delta p_b(\lambda^{(0)} + \epsilon_q)\alpha_b\gamma_b T_b^{(0)} + \Delta\bar{q}_b\omega_b^{(0)}] = 0, \quad (5.8g)$$

where we have used the lhs of the zeroth-order balances (5.8b–e) as well as (5.8f) to replace latent heating and moisture sink in the energy constraint. We note that small ($O(\tau_c)$) departures of T and q from adjustment to the reference profile yield order unity heating and moisture sink terms. This corresponds to balances hypothesized in a less formal framework by Arakawa and Chen (1987) with heating and moisture sink terms given diagnostically from the T and q equations. Since (5.8b–e) are needed only for the derivation of (5.8g), closure for the zeroth-order eigenvalue and variables is obtained at this order.

1) Propagating deep convective mode

For the case of $\lambda^{(0)} \neq -\epsilon_m$, (5.8a) holds with nonzero $T^{(0)}$ and $\omega^{(0)}$ and determines $\omega^{(0)}$ with only two vertical degrees of freedom (from the two constants of integration of $\partial_p^2\omega^{(0)}$ with $T^{(0)}$ given). This balance singles out a special vertical mode which turns out to be propagating (complex conjugate pair of eigenvalues, one of which is eliminated by y boundary conditions). Because of the great physical significance of this mode, we discuss it at length in section 5c.

2) Kinematically dominated modes

The propagating deep convective mode accounts for only two out of an infinite number of vertical degrees of freedom. To obtain the rest of the slow modes associated with these degrees of freedom while satisfying the constraint of the momentum equation, we are led to the case of $\lambda^{(0)} = -\epsilon_m$. This implies that the zeroth-order temperature and moisture components are zero and these modes are dominated by the kinematic variables, $\omega^{(0)}$ and $u^{(0)}$; hence, the term "kinematically dominated modes" is given to them. The first-order temperature and moisture variables enter the zeroth-order thermodynamic equations; the equations from the leading two orders of expansion are, in the troposphere:

$$T^{(0)} = T_c^{(0)} = T_b^{(0)} = 0, \quad (5.9a)$$

$$q^{(0)} = q_c^{(0)} = q_b^{(0)} = 0, \quad (5.9b)$$

$$(\partial_p\bar{S})\omega^{(0)} = (T_c^{(1)} - T^{(1)} - \Delta T_c^{(1)}), \quad (5.9c)$$

$$(\partial_p\bar{q})\omega^{(0)} = (\alpha\gamma T^{(1)} - q^{(1)}), \quad (5.9d)$$

$$T_c^{(1)} = A(p)h_b^{(1)}; \quad (5.9e)$$

while in the PBL they are

$$(\Delta\bar{S}_b/\Delta p_b)\omega_b^{(0)} = -\Delta T_c^{(1)}, \quad (5.9f)$$

$$(\Delta\bar{q}_b/\Delta p_b)\omega_b^{(0)} = (\alpha_b\gamma_b T_b^{(1)} - q_b^{(1)}). \quad (5.9g)$$

The zeroth-order thermodynamic variables are all unperturbed and the zeroth-order reference profiles of temperature and moisture are all zero. The kinematically dominated modes do not conform to conventional intuition about convectively adjusted dynamics in that the leading-order thermodynamic variables are not in adjustment with the reference profiles. These modes do obey "near-adjustment" constraints, but in the rather trivial sense that these leading-order, nonadjusted thermodynamic variables appear at $O(\tau_c)$ and are thus small. At zeroth order, the diabatic heating is balanced by the adiabatic cooling and the moisture sink is balanced by the moisture convergence. The energy constraint (5.8g) becomes

$$\int_{p_T}^{p_b}(\partial_p\bar{S} + \partial_p\bar{q})\omega^{(0)}dp + (\Delta\bar{S}_b + \Delta\bar{q}_b)\omega_b^{(0)} = 0. \quad (5.9h)$$

In the first term, $\partial_p\bar{S}$ (negative) dominates $\partial_p\bar{q}$ (positive) in the upper troposphere and $\partial_p\bar{q}$ dominates in the lower troposphere. In the second term, $(\Delta\bar{S}_b + \Delta\bar{q}_b)$ is positive. Thus, modes that have oscillatory structure in $\omega^{(0)}(p)$ that causes cancellation in the integral term will tend to have relatively small $\omega_b^{(0)}$, while modes that have less vertical structure must have sufficient amplitude of $\omega^{(0)}$ of the same sign as $\omega_b^{(0)}$ in the upper troposphere. We note that it is possible to enter higher-order dynamics to get $\lambda^{(1)}$, if desired; the case of $A(p)$ = const is outlined for illustration in appendix A. Again, we have a (countably infinite) set of modes, which are degenerate at leading order. This degeneracy will be broken if momentum diffusion is included but only in a manner similar to the diffusion equation. We therefore do not expect these modes individually to correspond to physical phenomena, although they will participate in the adjustment process from arbitrary initial conditions (or stochastically perturbed conditions).

c. Propagating deep convective mode (Madden–Julian mode)

Among the slow modes, a single mode stands out as having distinct properties and eigenvalue and is likely to have great physical significance. This mode is the only one for which the leading-order thermodynamics is in adjustment with reference profiles and is the only slow mode with zeroth-order thermodynamic quantities. The order τ_c^{-1} and order τ_c^0 balances are given by (5.7) and (5.8), respectively. Since all variables are zeroth order, we drop the superscripts hereafter for brevity. Thus, for the case of $\lambda^{(0)} \neq \epsilon_m$, the energy constraint (5.8g) can be rewritten as

$$(\lambda A^* + \epsilon^*)h_b = -\Delta p_T^{-1} \int_{p_T}^{p_b} (\partial_p \bar{h})\omega dp - (\Delta \bar{h}_b/\Delta p_T)\omega_b, \quad (5.10)$$

where

$$A^* = \hat{A} + \widehat{\alpha\gamma A} + \Delta p_b/\Delta p_T, \quad (5.11a)$$

$$\epsilon^* = \hat{A}\epsilon_r + (\Delta p_b/\Delta p_T)\epsilon_b. \quad (5.11b)$$

In (5.11b) we have set $\epsilon_q = \epsilon_b$ (same drag coefficient for evaporation and sensible heat). The quantity A^* provides a nondimensional measure of the thermal inertial of the motions associated with a given perturbation of h_b under the moist-adjusted constraints. Similarly, these constraints have implied that all forms of thermodynamic damping combine into the weighted vertical average, ϵ^*, which includes evaporative and sensible heat fluxes in the boundary layer in addition to radiative effects throughout the column. Equation (5.10) along with the zeroth-order momentum–continuity–hydrostatic equation,

$$(\lambda + \epsilon_m)\partial_p^2 \omega = \kappa(A(p)/p)k^2 h_b, \quad (5.12)$$

gives a complete system to be solved for slow mode solutions. We can integrate (5.12) to give

$$\omega = \frac{k^2 h_b}{(\lambda + \epsilon_m)} \kappa \int_p^{p_b} \int_{p'}^{p_b} A(p'')d\ln p'' dp' + \frac{(p_b - p)}{\Delta p_b}\omega_b + \omega_b, \quad (5.13)$$

where the first and second constants of integration have been chosen to satisfy the matching conditions at cloud base:

$$\omega|_{p_b} = \omega_b, \quad \partial_p \omega|_{p_b} = -\omega_b/\Delta p_b. \quad (5.14)$$

Substituting (5.13) into (5.10) yields

$$[(\lambda A^* + \epsilon^*)(\lambda + \epsilon_m) - M_P k^2]h_b - (\lambda + \epsilon_m)(\Delta p_T^{-1} + \Delta p_b^{-1})M_H \omega_b = 0, \quad (5.15)$$

where

$$M_P = -\frac{\kappa}{\Delta p_T} \int_{p_T}^{p_b} (\partial_p \bar{h}) \int_p^{p_b} \int_{p'}^{p_b} A(p'')d\ln p'' dp' dp, \quad (5.16a)$$

$$M_H = \frac{-1}{(\Delta p_T + \Delta p_b)} \int_{p_T}^{p_b} (p_b - p)(\partial_p \bar{h})dp + \frac{\Delta p_b}{(\Delta p_T + \Delta p_b)}(\bar{h}_b - \bar{h}_T). \quad (5.16b)$$

Both M_P and M_H are weighted vertical means of basic-state moist static stability. They provide measures of the net effects of stability on their respective parts of the moist, precipitating motions obeying the moist-adjusted constraints. The physical interpretation of M_P and M_H individually is less striking than that of the combination that arises when an upper boundary condition closes the problem as discussed below. We note that M_P comes from the *particular* solution to (5.13), which is directly driven by geopotential gradients implied by adjustment to the reference profile of temperature, while M_H comes from the *homogeneous* solutions in the heating region, which are implied by matching to the boundary layer. The second term, $(\bar{h}_b - \bar{h}_T)$, of M_H should be nearly zero since the cloud top is chosen such that $\bar{h}_{\text{sat}}|_{p_T} = h_b$, so that the basic-state moist static energy at cloud top is approximately equal to that of the PBL. It is noted that if the mean state were both moist adiabatic and saturated, $\partial_p \bar{h}$ would be zero. In a realistic basic state, the positive $\partial_p \bar{q}$ overcomes negative $\partial_p \bar{S}$ at low levels but the magnitude of $\partial_p \bar{S}$ is greater at upper levels. Signs are chosen such that both M_P and M_H are positive for realistic cases. An explicit form of (5.16a) is given for a special case in appendix C.

1) RIGID-LID CASE

Considering first the simple rigid-lid case, evaluating (5.13) at $p = p_T$, and applying the zero velocity condition yield

$$\widehat{A^+ k^2 h_b} + (\lambda + \epsilon_m)(\Delta p_T^{-1} + \Delta p_b^{-1})\omega_b = 0, \quad (5.17)$$

where $\widehat{A^+}$ is the vertical average of

$$A^+(p) = \kappa \int_p^{p_b} A(p)d\ln p'. \quad (5.18)$$

We note that A^+ gives the vertical structure of the geopotential gradients associated with quasi-equilibrium temperature perturbations, relative to a reference level at cloud bottom. In (5.17), the $\widehat{A^+}$ term is thus associated with the contribution of these toward the vertical velocity at p_T. For nontrivial solutions, (5.15) and (5.17) require

$$(\lambda + \epsilon_m)[(\lambda A^* + \epsilon^*)(\lambda + \epsilon_m) + \Delta M k^2] = 0. \tag{5.19}$$

This indicates the possible root of $\lambda^{(0)} = -\epsilon_m$, which has been discussed earlier. The other two possible propagating roots are

$$\lambda = -\frac{1}{2}(\epsilon_m + \epsilon^*/A^*) \pm \frac{1}{2} i[(4\Delta M/A^*)k^2 - (\epsilon_m - \epsilon^*/A^*)^2]^{1/2}. \tag{5.20}$$

In (5.19) and (5.20), we have defined

$$\Delta M = \hat{A}^+ M_H - M_P, \tag{5.21}$$

which represents the net static stability, including moist effects, in the troposphere felt by this mode. This was termed the gross moist stability by Neelin and Held (1987) where it was defined in a two-level model for the steady tropical circulation. A time-dependent version of the same two-level model was used by Neelin et al. (1987); it is remarkable that the dispersion relation for this mode is *identical in form to the two-level case,* but with a *precise meaning* given to the *gross moist stability* and to the *net thermodynamic damping.*

The mode is oscillatory as long as the damping is not too large compared to the propagation tendency from the gross moist stability term; that is,

$$(4\Delta M/A^*)k^2 > (\epsilon_m - \epsilon^*/A^*)^2. \tag{5.22}$$

Care is needed in estimating ΔM since $\partial_p \bar{S}$ and $\partial_p \bar{q}$ oppose each other. An estimate of ΔM from the basic state in Fig. 1 using (5.16a) and (5.16b) suggests a value of about 180 J kg^{-1}. Using the linear approximation to $A(p)/p$ of (C.3) in M_P yields values in the range from 150 to 100 J kg^{-1}.

Using $\epsilon_m = \epsilon_r = (10 \text{ days})^{-1}$, $\alpha = 0.8$, $\Delta p_T = 825$ mb, and $\Delta p_b = 75$ mb suggests that condition (5.22) can be satisfied to very small wavenumber ($\approx$0.1). Defining

$$C = \frac{1}{2k}[(4\Delta M/A^*)k^2 - (\epsilon_m - \epsilon^*/A^*)^2]^{1/2} \tag{5.23}$$

gives the zonal phase speed for this mode (including damping effects). The eastward propagating case [negative root in (5.20)] is appropriate to the Kelvin wave; the westward case is appropriate for the long Rossby waves, with k rescaled by $(2n + 1)$.

Since the MJO is characterized by Kelvin wave–like structures and is dominated by planetary wavenumbers, we focus on the wavenumber one Kelvin wave case. Figure 3 shows the normalized vertical profiles of vertical velocity, latent heating, and moisture sink from the eigenvector reconstructed from the solution (5.13) for ω, using the moist adiabat reference profile for $A(p)$. The profiles exhibit deep convective structures with latent heating balanced by moisture sink. It is noted that these profiles are determined *internally* by the *dynamics* and do not resemble the vertical dependence of the reference profile. The position of maximum vertical velocity and latent heating is around 500 mb and the position of maximum moisture sink is lower than the latent heating peak, reflecting the vertical redistribution of heating by convection.

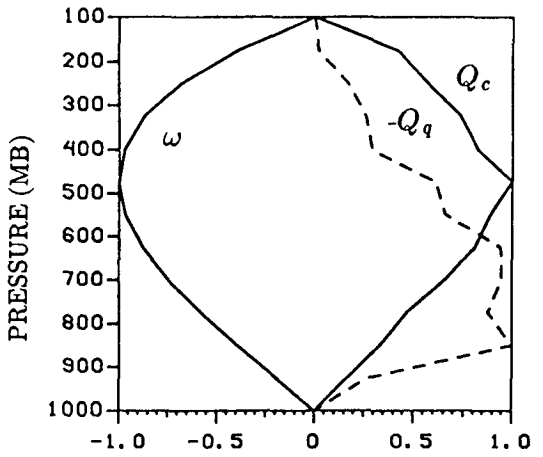

FIG. 3. Vertical profiles of normalized pressure velocity, latent heating, and moisture sink for the propagating deep-convective mode (Madden–Julian mode) from the analytical solutions (5.13) using the moist-adiabat reference profile.

Estimates of (5.20) using previously mentioned parameter values give a decay rate of about (13 days)$^{-1}$ and a period of about 31 days for wavenumber one (see appendix C for a discussion of sensitivity). Since this wavenumber one propagating deep convective mode has vertical structures and period very similar to the eastward propagating MJO appearing in many GCM studies, the term "Madden–Julian (MJ) mode" will sometimes be used. The decay rate of the MJ mode, at this order in τ_c, is determined by a weighted combination of physical damping effects, ϵ_m, ϵ_r, and ϵ_b, and for typical parameters this is smaller than the mechanical damping rate. If these damping rates are all small, this mode is near neutral at this order, but next-order corrections introduce an additional damping due to τ_c. The period of the MJ mode is mainly determined by the gross moist stability, ΔM, as suggested in (5.20).

2) RADIATION UPPER BOUNDARY CONDITION CASE

Here we discuss the impact of a more realistic upper boundary condition on the MJ mode. The formulation of the radiation condition is given in appendix B, where its effect upon other modes is qualitatively discussed. Hayashi (1971b) stated that there is no significant difference between rigid-lid and radiation upper boundary conditions for the tropical-trapped waves in a CISK model using Kuo-like scheme when the heating is sufficient large. Recently, Yano and Emanuel (1991) indicated that a scale selectivity can result from the use of a radiation upper condition.

Evaluating (5.13) at $p = p_T$ yields

$$\frac{\widehat{A^+}}{(\lambda + \epsilon_m)} k^2 h_b + (\Delta p_T^{-1} + \Delta p_b^{-1})\omega_b - \Delta p_T^{-1}\omega_T = 0, \quad (5.24)$$

where ω_T is the vertical velocity at cloud top. The radiation condition, (B.3), gives

$$\frac{A_T^+}{(\lambda + \epsilon_m)} k^2 h_b + \frac{1}{\Delta p_b}\omega_b + \frac{1}{(\lambda + \epsilon_m)} \frac{N}{(\Delta p_b + \Delta p_T)}\omega_T = 0, \quad (5.25)$$

where $A_T^+ = A^+(p_T)$ and

$$N = \begin{cases} \text{sgn}[\text{Re}(\lambda + \epsilon_m)](\Delta p_b + \Delta p_T)[\kappa(-\partial_p \bar{S})/p_T]^{1/2}k, & \text{for stationary waves} \\ (\Delta p_b + \Delta p_T)[\kappa(-\partial_p \bar{S})/p_T]^{1/2}k, & \text{for propagating waves.} \end{cases}$$

The quantity N is proportional to the large Brunt–Väisälä frequency of the stratosphere with a form similar to that of a gravity wave with large vertical wavelength; it is of order 10^{-4} s^{-1}, which is large compared to the tropical low-frequency oscillation. The system (5.24), (5.25), and (5.15) yields

$$\lambda^3 + (N + \epsilon^*/A^* + 2\epsilon_m)\lambda^2 + [(\epsilon_m + \epsilon^*/A^*)(N + \epsilon_m) + \epsilon_m\epsilon^*/A^* + k^2(\Delta M + \Delta M^R)/A^*]\lambda + \{(\epsilon_m\epsilon^*/A^* + k^2\Delta M/A^*)N + \epsilon_m[\epsilon_m\epsilon^*/A^* + k^2(\Delta M + \Delta M^R)/A^*]\} = 0, \quad (5.26)$$

where we have defined a positive quantity similar to the gross moist stability but due to the additional effects of the radiation condition:

$$\Delta M^R = [\widehat{A^+} + (1 + \Delta p_b/\Delta p_T)A_T^+]M_H. \quad (5.27)$$

Equation (5.26) appears to contain three roots of λ, but in fact one of them is excluded by the dependence of N on sign(λ) in the radiation boundary condition. To obtain the qualitative behavior of (5.26), an expression of λ in orders of the small parameter N^{-1} is used. Considering a leading term $\lambda^{(-1)}$, the leading-order [$O(N^3)$] balance gives either $\lambda^{(-1)} = 0$ or $\lambda^{(-1)} = -1$. The latter violates the radiation boundary condition for the stationary waves and is not a true solution.

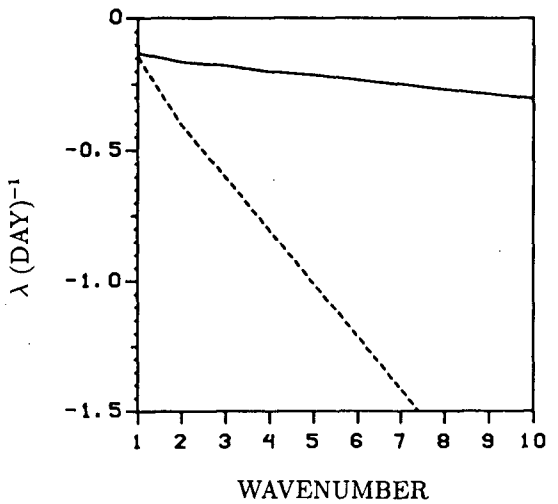

FIG. 4. The eigenvalue of Madden–Julian mode with a radiation upper boundary condition as a function of zonal wavenumber. Solid line denotes growth rate and dashed line denotes frequency.

For the case of $\lambda^{(-1)} = 0$, the leading-order [$O(N)$] balance gives exactly the same dispersion relation as that in the rigid-lid case, that is, (5.20), for the MJ mode, which evolves slowly at O(1). Thus, the behavior of MJ mode is not qualitatively modified by the radiation boundary condition. However, as pointed out by Yano and Emanuel (1991), a scale selectivity can result from this effect. The next-order dispersion relation, derived from the O(1) balance, gives

$$\lambda^{(1)} = -\left[\frac{1}{2} + \frac{(\epsilon_m - \epsilon^*/A^*)}{4kC} i\right] \frac{\Delta M^R}{A^*} k^2, \quad (5.28)$$

where we have chosen the sign for Kelvin wave propagation. An estimate of (5.28) shows that $\text{Re}(\lambda^{(1)}) < 0$ and $\text{Im}(\lambda^{(1)}) > 0$ for eastward propagation. Thus, the effect of the radiation condition tends to stabilize the wave and slow down its phase speed. From (5.28), it may be seen that the stabilization due to the radiation condition is independent of thermal or mechanical damping, whereas the phase speed modification depends on the interaction of these with the radiation condition. Figure 4 shows the impact of the radiation condition on the propagating deep convective mode from a numerical solution of (5.26). The additional stabilization of the wave by the radiation condition is modest at wavenumber 1, with decay time of about 8 days compared to 13 days in the rigid-lid case. However, the radiation condition introduces significant scale selectivity in favor of planetary scales by strongly damping higher wavenumbers. The slowing of the phase speed by the radiation condition yields a period of 43 days at wavenumber 1 compared to 31 days in the rigid-lid case.

d. Inclusion of evaporation–wind feedback

In the above analysis, we temporarily neglect the evaporation–wind feedback. When the evaporation–

wind feedback term in (3.12) is added, for the Kelvin wave case, the dispersion relation (5.20) becomes

$$\lambda = -\frac{1}{2}(\epsilon_m + \epsilon^*/A^*) - i(C^2k^2 - iF^*k)^{1/2}, \quad (5.29)$$

where $F^* = F[gL(\widehat{A^+}/A^*)(\Delta p_T + \Delta p_b)^{-1}]$ is the redefined evaporation–wind feedback parameter in units of J kg^{-1} m^{-1} and we have chosen the sign appropriate to Kelvin wave propagation. Alternatively, (5.29) can be expressed as

$$\lambda = -\frac{1}{2}(\epsilon_m + \epsilon^*/A^*) + \frac{1}{\sqrt{2}}Ck[(1 + F^{*2}C^{-4}k^{-2})^{1/2} - 1]^{1/2} - i\frac{1}{\sqrt{2}}Ck[(1 + F^{*2}C^{-4}k^{-2})^{1/2} + 1]^{1/2}. \quad (5.30)$$

From (5.30), it is clearly seen that the eastward moving Kelvin wave is destabilized (real part of the eigenvalue increased) by the inclusion of evaporation–wind feedback while the period decreases with increasing F^*. If a westward propagating anti–Kelvin wave solution were permitted, it would be stabilized by the evaporation–wind feedback. As noted in Neelin et al. (1987), the growth rate asymptotes to a constant value at large k, that is,

$$\lambda \to \frac{1}{2}[(\Delta M/A^*)^{-1/2}F^* - (\epsilon_m + \epsilon^*/A^*)], \quad (5.31)$$

so there is no strong scale selectivity in this dispersion relation, although at least it avoids selecting the smallest scales, as is common in CISK models. Scale selectivity can be produced either by including the radiation upper boundary condition, or by the effects of finite τ_c (as will be addressed in Part II). When the evaporation–wind feedback is large enough, the Kelvin mode becomes unstable. This is the only case where the nonlinear terms in (2.1) are required to obtain an equilibrated solution. This fulfills the conditions for a simple Hopf bifurcation since the nonlinear terms are smooth functions of the large-scale variables in the vicinity of the RCE; Re(λ) increases with F^*; and, when scale selectivity is included, a single wavelength goes unstable at a critical value of F^*. The weakly nonlinear solutions for slightly supercritical F^* will be pursued in further work. We anticipate that the nonlinearity from $\mathcal{N}_{q_b}$ alone will be sufficient to equilibrate the instability.

6. Conclusions

Conclusions from these results may be drawn at two levels: first, a series of results on how a model atmosphere behaves under moist convective adjustment (MCA), which are novel but rather specific. Second, we elaborate the discussion to more general implications both for modeling studies and for the tropical atmosphere. The former can be exactly defended for particular cases, while the latter takes MCA as a prototype of convectively imposed thermodynamic constraints and considers the view of tropical dynamics implied by this.

a. Summary

We examine the modes of the tropical atmosphere that arise from convection—as represented by a smoothly posed MCA scheme that follows Betts–Miller (1986)—interacting with large-scale dynamics. In this version of MCA, the effects of deep cumulus convection are parameterized as adjusting the large-scale temperature and moisture fields toward reference profiles, which are functions of the large-scale thermodynamic variables. The reference temperature profile is related to the moist adiabat rising from the boundary layer and thus depends on variations of the boundary-layer moist enthalpy, while the moisture reference profile is related to a given degree of subsaturation. The results prove rather insensitive to the details of these profiles, and some simplifications to the Betts–Miller scheme are made. What makes Betts–Miller MCA appealing, and permits this type of analysis to be carried out for the first time with a MCA scheme, is that the thermodynamic fields are relaxed toward their adjusted state smoothly on a time scale τ_c, typical of cumulus ensemble life cycles. While many of the results obtained here may be expected to carry over to classical Manabe MCA, some aspects may differ. In practice, a GCM running classical MCA adjusts a few levels at a time, and it may take a considerable number of time steps to adjust an entire column (Manabe 1991, personal communication; Hess et al. 1992); often, saturation criteria must be met in addition to column stability criteria.

In Part I of this paper, we exploit the fact that the cumulus time scale is much shorter than planetary-scale dynamical time scales to obtain analytical results by asymptotic methods. The main findings of this approach are:

1) *Two main classes of mode are found under MCA:* "fast modes," which decay on the order of the adjustment time scale, τ_c, and "slow modes," which have time scales set by the large-scale dynamics. This has several implications that are consistent with intuition about how MCA works. If one considers the initial value problem of adjustment from initial conditions, the fast modes will rapidly adjust the atmosphere toward a state that obeys the convective adjustment constraints up to first order in τ_c, leaving the part of the initial conditions, which projects on the slow modes, to evolve on longer time scales. These fast modes are in some sense MCA's representation of the net effect on

large scales of the full life cycle of convective ensembles growing through convective instability (of the "first kind," i.e., conditional instability within columns) and equilibrating through removal of the column instability. That these modes are all rapidly decaying implies that, although the MCA representation might be crude in some respects, at least it mitigates the danger that subgrid-scale convective instability of the first kind will be expressed at large scales. For a nonlinear or stochastically forced problem, the solution may be expected to be dominated by slow modes, with a contribution due to fast modes only of order τ_c. The slow modes obey near-adjusted thermodynamical constraints to order τ_c, so any long-term solution must be in convective adjustment to this order. As long as the reference profiles are not too different from moist adiabatic, the degree of MAE (moist available energy) in precipitating regions will be small in a model running MCA, consistent with Randall and Wang (1992).

2) *Fast mode characteristics:* the balances are, as one would expect for such fast-decaying modes, between time rate change of temperature (moisture) and latent heating (moisture sink), with little role for adiabatic cooling (moisture convergence). While the fast modes are not of direct geophysical interest, it is worth noting some properties for the sake of possible insight into numerical behavior. A large subclass of the fast modes are degenerate to a first approximation, all decaying at rate τ_c^{-1}. These modes will thus never be seen individually and convective adjustment of anomalies that are associated with these will tend to occur locally, a numerically desirable feature.

3) *Among the slow modes, two classes of mode are found:* a single vertical mode that obeys special balances and is the most physically interesting—the "propagating deep convective mode," discussed below. The rest of the vertical modes decay at a rate dictated by purely mechanical damping. These modes are dominated by the kinematic variables, and the energy balances of these "kinematically dominated modes" are exactly between latent heating and adiabatic cooling at leading order. Since the zeroth-order thermodynamic variables are all unperturbed, these modes obey near adjustment to the reference profiles in a rather trivial manner. They are of little geophysical interest but of some numerical concern since they decay slowly. The structure of these modes and the fast modes will be touched on in Part II.

4) The propagating deep convective mode is the only vertical mode consistent with intuition about large-scale flow evolving subject to convective adjustment—indeed, the leading-order balances correspond to balances postulated on physical grounds by Arakawa and Chen (1987) for classical convective adjustment—although it would be difficult to guess a priori that only a single vertical mode could satisfy these constraints or that classical adjustment represents a singular limit. Because the temperature profile is constrained to the reference profile at leading order, the combined hydrostatic, continuity, and momentum equations lead to a solution for vertical velocity throughout the troposphere that has only two vertical degrees of freedom. Upon application of matching conditions and energy constraint, this leads to a single complex conjugate pair of eigenvalues, one of which is eliminated by y boundary conditions. The mode has deep convective structure, which depends relatively little on the vertical structure of the reference profile. The thermodynamic balances involve strong cancellation of adiabatic cooling (moisture convergence) and diabatic heating (moisture sink), but do also have temperature and moisture tendencies at leading order.

Remarkably, the analysis leads to a well-defined gross moist stability for the mode, which dictates its slow phase speed. The idea of a gross moist stability representing an effective static stability for the troposphere for deep convective motions was employed by Neelin and Held (1987) and is easily defined in a two-level model, such as that used for the MJO by Neelin et al. (1987), but had previously not been well defined in a vertically continuous model. Here the gross moist stability is given in terms of vertical integrals over thermodynamic basic-state quantities. A net thermodynamic damping time due to mechanisms from both temperature and moisture equations may be similarly defined in terms of vertical integrals. For typical parameters, the damping rate of this mode is smaller than the mechanical damping time scale. The dispersion relation for the mode, carried to order unity in τ_c, turns out to be mathematically identical to that of the two-level model.

5) For a given vertical mode, there is a set of meridional modes with structures given in terms of Hermite functions. Since the propagating deep convective mode is unique, we can refer to the corresponding modes as Rossby and Kelvin modes without confusion (where necessary, "moist Rossby" and "moist Kelvin" mode will be used); obviously the meridional scales are determined by the radius of deformation defined using the moist phase speed, and are hence smaller than would be the case for dry wave motions. The moist Kelvin mode has obvious parallels to the Madden–Julian Oscillation, as pointed out by a number of earlier studies. For wavenumber one, the Kelvin propagating deep convective mode has period of about 43 days for reasonable parameters (31 days for the rigid-lid case), consistent with MJO time scales. The vertical structure of the Madden–Julian mode in this model exhibits significant parallels to the vertical structure of the observed MJO and that found in GFDL GCM (Lau et al. 1988). While we do not have a clear-cut answer to the question of why the phase speed in the GFDL GCM is too fast, the slowing that occurs when a radiation upper boundary condition is used, relative to the rigid-lid case, is suggestive.

6) We find that for any reasonable vertical structure of the homogeneous basic state, all large-scale modes are stable under MCA interacting with dynamics. However, the MJ mode (Kelvin deep convective mode) can be destabilized by the inclusion of the evaporation–wind feedback. Scale selectivity can occur through preferential upward radiation of shorter-scale waves when a radiation upper boundary condition is used. The use of the small τ_c expansion in the analytic results considered here restricts their application to wavenumbers larger than those where dynamical time scales approach τ_c (for a phase speed of 14 m s^{-1}, this assumption will begin to fail for wavenumber on the order of 10, for $\tau_c = 2$ h). Scale selectivity due to further damping of high wavenumbers by the effects of finite τ_c will be discussed in Part II.

b. *Discussion*

In discussing the above results, we encounter a problem of terminology that has been plaguing the field for some time. While the collective effects of convection interacting with large-scale dynamics are clearly fundamental to many tropical phenomena, there is no generic term by which to refer to this. Given this lack, "CISK" is often used to refer to such phenomena, either observed or in GCMs, even though conditional instability of the second kind may play no role in maintaining them (in the sense of MAE providing a net energy source to the large scales). Since CISK in this strict sense is coming increasingly into question (Betts 1982; Xu and Emanuel 1989; Randall and Wang 1992), we suggest that it is useful to introduce a more accurate terminology. Following discussions with a number of other investigators, we propose that "convective interaction with dynamics" (CID)[1] would be a suitable generic term for all such interactions, regardless of the stability properties, linearity or nonlinearity, etc. It can be applied to all horizontal scales large enough that convection can sensibly be thought of as having a collective effect on the dynamics.

The simple linear CID problem considered here provides an example where the distinction is both useful and obvious. For Betts–Miller MCA interacting with large-scale dynamics, CID dominates the linear modes to such an extent that they have no close relation to modes of the dry atmosphere—but, nonetheless, no CISK is present. Our results concur with a number of previous CID studies (Lindzen 1974; Lau and Peng 1987; Chang and Lim 1988; Lau et al. 1988; Sui and Lau 1989) that Kelvin wave CID determines both the structure and phase speed of the Madden–Julian Oscillation. They disagree with some of these studies that CISK is the best candidate as a mechanism for destabilizing it. However, we note that our current results are for a horizontally homogeneous basic state and that we cannot exclude the possibility that CISK may arise if the basic state has sufficiently strong horizontal gradients. The evaporation–wind feedback has been shown to destabilize the Kelvin–CID mode and so provides a maintenance mechanism for the MJO, which is known to be relevant in some GCMs. Alternate mechanisms involving stochastic forcing of the weakly damped Kelvin–CID mode either by other tropical variance or from midlatitudes (Hsu et al. 1990) are discussed in Part II.

In general, we suggest that insofar as linear theory can be applied, MCA CID will tend to differ from Kuo-like CID in three main respects. (i) The propagating deep-convective mode is unique in MCA CID, whereas Kuo-like CID tends to have a sequence of vertical modes with less qualitative difference in their properties. (ii) Kuo-like CID can easily exhibit CISK especially if the heating profile is specified independently from the basic state; MCA CID will tend not to exhibit CISK except possibly under specialized conditions. (iii) Wavenumber dependences and scale selectivity will differ markedly, especially with respect to CISK aspects. This will be elaborated on in Part II. MCA CID and Arakawa–Schubert CID are more similar with respect to the lack of CISK. Overall, the CID properties of the deepest mode will tend to be rather similar among all three schemes in terms of structure, balances, and propagation characteristics. In other words, some of the most geophysically important aspects of simple linear CID modes tend to be robust to the choice of convective scheme, while CISK appears to be very sensitive to this choice.

A major difference of MCA CID compared to Kuo-like CID is the form of the nonlinear behavior that may be expected. The current scheme has smooth nonlinear terms in a neighborhood of the RCE (radiative–convective equilibrium) and is inherently stable unless the evaporation–wind feedback is large. This satisfies conditions for a weakly nonlinear treatment of large-scale variability, in particular the MJO, directly in terms of the large-scale variables, in contrast to examples of Kuo-like CID (e.g., Lau and Peng 1987) where nonlinearly equilibrated small scales must typically be included in the resolved dynamics.

Discussion of these differences requires explicit consideration of the role of the Reynolds average in convective parameterization (the assumed time and space average over small-scale motions to define the ensemble whose effects on the larger scales is parameterized; e.g., Yanai et al. 1973). In formulating a parameterization, it is not clear in advance which

[1] CID appears to be the winner over a number of suggested acronyms, including DICE (dynamics interacting with convective ensembles), CILD (convective interaction with large-scale dynamics), CILC (convection interacting with the large-scale circulation), and CECIL (collective effects of convection interacting with large scales). Goswami and Goswami (1991) have used "interaction between convection and dynamics."

phenomena will be completely subsumed into the sub-Reynolds scales (i.e., have their effects represented entirely by the parameterization as a function of the large-scale flow), and which phenomena will be expressed in the explicitly modeled large-scale flow. In a gridpoint model, these will correspond to subgrid scale and resolved scales, respectively; we use sub- and supra-Reynolds scales for generality and because the terms small and large scale can be ambiguous. When interaction of the supra-Reynolds scales with a cumulus parameterization is examined, some schemes tend to produce features at the smallest resolved scale, which are cloudlike in the sense that they grow from the MAE of the large scales—in other words, column conditional instability is to some degree being directly expressed in the resolved motions. In the case of smoothly formulated MCA, on the other hand, we have a clear-cut example where column conditional instability is entirely expressed at sub-Reynolds scales. The flow in our case evolves about an RCE that is everywhere continually being destabilized (in terms of production of MAE or column conditional instability) by evaporation and radiative cooling, but this does not destabilize the supra-Reynolds scales because the MAE is continuously being "eaten up" at the sub-Reynolds scales. Convection and rain occur everywhere due to the net effects of motions at the sub-Reynolds scales, but the small amount of MAE left over does not lead to any growth at supra-Reynolds scales (i.e., no CISK).

This might imply, on the one hand, that this scheme is not entirely suitable for studying some of the smaller-scale features of tropical meteorology, like squall lines, but from the point of view of the theory of tropical large-scale dynamics, it is a fortunate property. The thermodynamic quasi-equilibrium constraints imposed on the supra-Reynolds scales by the net effects of convection strongly affect the large-scale phenomena. The way that this occurs under smooth MCA provides a very useful theoretical tool: the stability properties of the analysis presented here lay the groundwork for approximations that retain only motions that satisfy quasi-equilibrium constraints. Furthermore, they suggest that this approach can provide a self-consistent system for directly studying the large scales, as they evolve subject to these convective quasi-equilibrium constraints, without necessarily having to resolve any cascade of unstable motions at scales between the Reynolds scale and the scales of interest. In short, smoothly posed MCA provides a way of looking at the convection, in its interaction with supra-Reynolds-scale dynamics, as a forest rather than as a large number of highly nonlinear trees. We conjecture that this view can be extended to other convective schemes based on quasi-equilibrium thermodynamic closures.

In Part II of this paper, we take the next step in establishing this approach for the case of MCA by considering what happens at small (but supra-Reynolds) scales and the spectrum of large-scale variance that would be maintained by stochastic forcing associated with sub-Reynolds-scale motions.

Acknowledgments. This work was supported in part by NSF Grant ATM-9215090. One of the authors (JYY) was also supported in part by a postgraduate scholarship from the Ministry of Education, Republic of China. It is a pleasure to acknowledge discussions with A. Arakawa, A. Betts, C. Bretherton, K. Emanuel, Y. Hayashi, I. Held, N.-C. Lau, S. Manabe, R. Lindzen, and M. Yanai.

APPENDIX A

Order τ_c Eigenvalue, $\lambda^{(1)}$, for Kinematically Dominated Modes

The momentum equation of slow kinematically dominated modes at order τ_c balance is

$$\lambda^{(1)}\partial_p^2\omega^{(0)} = (\kappa/p)k^2T^{(1)}. \tag{A.1}$$

With the aid of (5.9c), (5.9f), (5.9g), and (5.9e), Eq. (A.1) can be expressed as

$$\frac{p}{k^2}\lambda^{(1)}\partial_p^2\omega^{(0)} + \kappa(\partial_p\bar{S})\omega^{(0)} = A(p)h_b^{(1)} + (\partial_p\bar{S} - A(p)\partial_p\bar{q})|_b\omega_b^{(0)}. \tag{A.2}$$

Homogeneous solutions have a vertical wavenumber approximately given by $m^2 = \kappa(\partial_p\bar{S}/p)k^2/\lambda^{(1)}$ where $\lambda^{(1)}$ has dimension of s^{-2}. For the case where $A(p)$, $\partial_p\bar{S}/p$, and $\partial_p\bar{q}$ are constants, and neglecting compressibility effects, (A.2) gives

$$\omega^{(0)} = \left[\frac{A(p)}{\partial_p\bar{S}}h_b^{(1)} + \frac{(\partial_p\bar{S} - A(p)\partial_p\bar{q})|_b}{\partial_p\bar{S}}\omega_b^{(0)}\right] \times [1 - \cos m(p - p_T)] + C\sin m(p - p_T), \tag{A.3}$$

where we have used the rigid-lid condition, $\omega = 0$, at cloud top since the radiation condition reduces to the rigid-lid condition to order $\tau_c^{1/2}$ for these modes. Applying cloud-base matching conditions in (A.3) as well as using (A.3) in the energy constraint (5.8g) yields a set of equations for m. These quantization conditions give a series of discrete, finite m^2, and hence $\lambda^{(1)}$. The structures of these modes are then determined at this order. The eigenvalues are degenerate at leading order $\lambda^{(0)} = -\epsilon_m$ but even as $\tau_c \to 0$, the vertical structures remain unchanged and distinct. The value of $\lambda^{(1)}$ tends to be negative, that is, these modes damp slightly faster than the mechanical damping time, as we shall see numerically in Part II.

APPENDIX B

The Radiation Upper Boundary Condition

Above the heating, the perturbation in the stratosphere obeys

$$(\lambda + \epsilon_r)(\lambda + \epsilon_m)\partial_p^2\omega + \kappa(\partial_p\bar{S}/p)k^2\omega = 0. \quad \text{(B.1)}$$

Neglecting compressibility, for solutions of the form $\omega = \omega_T \exp[\mu(p - p_T)]$ where ω_T is the pressure velocity at the top of the heating and μ is defined as

$$\mu^2 = \frac{\kappa(-\partial_p\bar{S}/p_T)}{(\lambda + \epsilon_r)(\lambda + \epsilon_m)} k^2. \quad \text{(B.2)}$$

Choosing the vertically decaying or upward energy propagation root for μ yields the radiation condition:

$$\omega_T = \frac{1}{\mu} \partial_p\omega|_{p=p_T}, \quad \mathrm{Re}(\mu) > 0, \quad \text{(B.3)}$$

where the rhs is evaluated from the solution below the top of the heating. Equation (B.3) approaches the simplifying rigid-lid condition when μ is sufficiently large. For those modes having $\lambda \to \epsilon_m$, the value of μ tends to be large. Thus, surprisingly, the kinematically dominated modes are little affected by the presence or absence of a lid. The fast-decaying modes will have substantial penetration into the stratosphere, but their leading-order behavior is dictated by the convective processes. Thus, the only mode significantly affected by the lid is the propagating deep convective mode, as discussed in section 5.

APPENDIX C

Case of a Linear $A(p)/p$ Profile

A special case that permits explicit evaluation of the double integrals in M_P, ω, etc., occurs if we let the coefficient of k^2h_b in (5.12) linearly increase with height; that is,

$$\kappa \frac{A(p)}{p} = \frac{(p_b - p)}{\Delta p_T^2} A_s + \frac{A_b}{\Delta p_T}, \quad \text{(C.1)}$$

where A_s is a unitless constant for the slope and $A_b = \kappa(1 + \gamma_b)^{-1}\Delta p_T/p_b$ is the cloud-base value given by $A(p_b) = (1 + \gamma_b)^{-1}$. Then (5.13) becomes

$$\omega = \left[\frac{A_s}{6\Delta p_T^2}(p_b - p)^3 + \frac{A_b}{2\Delta p_T}(p_b - p)^2\right] \times \frac{k^2}{(\lambda + \epsilon_m)} h_b + \frac{(p_b - p)}{\Delta p_b}\omega_b + \omega_b \quad \text{(C.2)}$$

and (5.16a) and $\hat{A}^+$ become

$$M_P = -\frac{A_s}{6\Delta p_T^3}\int_{p_T}^{p_b}(p_b - p)^3(\partial_p\bar{h})dp - \frac{A_b}{2\Delta p_T^2}\int_{p_T}^{p_b}(p_b - p)^2(\partial_p\bar{h})dp, \quad \text{(C.3)}$$

$$\hat{A}^+ = A_s/6 + A_b/2. \quad \text{(C.4)}$$

Note that the weighting by $(p - p_b)^n$, $n = 2, 3$ in the various terms of M_P emphasizes the upper levels more than the linear weighting in M_H given by (5.16b). For $A_s = 2.5$, the first term of (C.3) accounts for 80% of M_P; while for $A_s = 1.5$, the first term of (C.3) accounts for 70% of M_P. Despite the crude approximation to the profile, the vertical structures implied by (C.2) (Fig. C1) are remarkably similar to the exact calculations (Fig. 3), an indication that this structure is very robust. For $A_s = 2.5$, 1.5 (see Fig. 2), the period at wavenumber 1 is 34 days and 44 days, respectively, compared to 31 days for the moist adiabat. Since these represent large changes to the reference temperature profile, we conclude that the eigenvalue is not highly sensitive to this profile, but that it may have some quantitative impact.

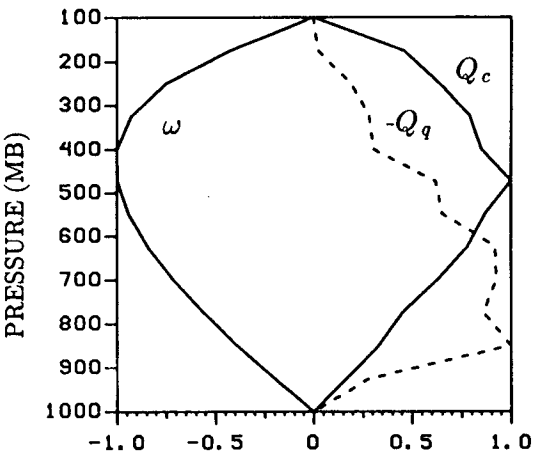

FIG. C1. Same as Fig. 3 except that these profiles are calculated from (C.2) using the linear approximation to the $A(p)/p$ structure with $A_s = 2.5$.

REFERENCES

Arakawa, A., and W. H. Schubert, 1974: Interaction of a cumulus cloud ensemble with the large-scale environment, Part I. *J. Atmos. Sci.*, **31**, 674–701.

——, and J. Chen, 1987: Closure assumptions in the cumulus parameterization problem. *Collection of Papers Presented at the WMO/IUGG Symp. on Short- and Medium-Range Numerical Weather Prediction*, Tokyo, 107–131.

Betts, A. K., 1982: Saturation point analysis of moist convective overturning. *J. Atmos. Sci.*, **39**, 1484–1505.

——, 1986: A new convective adjustment scheme. Part I: Observational and theoretical basis. *Quart. J. Roy. Meteor. Soc.*, **112**, 677–691.

——, and M. J. Miller, 1986: A new convective adjustment scheme. Part II: Single column tests using GATE wave, BOMEX, ATEX and arctic air-mass data sets. *Quart. J. Roy. Meteor. Soc.*, **112**, 693–709.

Chang, C. P., 1976: Vertical structure of tropical waves maintained by internally-induced cumulus heating. *J. Atmos. Sci.*, **33**, 729–739.

——, 1977: Viscous internal gravity waves and low-frequency oscillation in the tropics. *J. Atmos. Sci.*, **34**, 981–991.

——, and T. M. Piwawar, 1974: Effect of a CISK parameterization on tropical wave growth. *J. Atmos. Sci.*, **31**, 1256–1261.

——, and H. Lim, 1988: Kelvin wave–CISK. A possible mechanism for the 30–50 day oscillations. *J. Atmos. Sci.*, **45,** 1709–1720.

Charney, J. G., and A. Eliassen, 1964: On the growth of the hurricane depression. *J. Atmos. Sci.*, **21,** 68–74.

Crum, F. X., and D. E. Stevens, 1983: A comparison of two cumulus parameterization schemes in a linear model of wave–CISK. *J. Atmos. Sci.*, **40,** 2671–2688.

Davies, H. C., 1979: Phase-lagged wave–CISK. *Quart. J. Roy. Meteor. Soc.*, **105,** 325–353.

Emanuel, K. A., 1987: An air–sea interaction model of intraseasonal oscillations in the tropics. *J. Atmos. Sci.*, **44,** 2324–2340.

Goswami, P., and B. N. Goswami, 1991: Modification of $n = 0$ equatorial waves due to interaction between convection and dynamics. *J. Atmos. Sci.*, **48,** 2231–2244.

Guckenheimer, J., and P. Holmes, 1983: *Nonlinear Oscillations, Dynamical System and Bifurcations of Vector Fields.* Springer-Verlag, 459 pp.

Hayashi, Y., 1970: A theory of large-scale equatorial waves generated by condensation heat and accelerating the zonal wind. *J. Meteor. Soc. Japan,* **48,** 140–160.

——, 1971a: Instability of large-scale equatorial waves with a frequency-dependent CISK parameterization. *J. Meteor. Soc. Japan,* **49,** 59–62.

——, 1971b: Instability of large-scale equatorial waves under the radiation condition. *J. Meteor. Soc. Japan,* **49,** 316–319.

——, 1971c: Large-scale equatorial waves destabilized by convective heating in the presence of surface friction. *J. Meteor. Soc. Japan,* **49,** 458–466.

Hayashi, Y. Y., and A. Sumi, 1986: The 30–40 day oscillations simulated in an 'aqua planet' model. *J. Meteor. Soc. Japan,* **64,** 451–466.

Hess, P. G., D. S. Battisti, and P. J. Rasch, 1993: The maintenance of the intertropical convergence zones and the large-scale tropical circulation on a water-covered earth. *J. Atmos. Sci.*, **50,** 691–713.

Hsu, H. H., B. J. Hoskins, and F. F. Jin, 1990: The 1985/86 intraseasonal oscillation and the role of the extratropics. *J. Atmos. Sci.*, **47,** 823–839.

Krishnamurti, T. N., P. K. Jayakumar, J. Sheng, N. Surgi, and Kurma, 1985: Divergent circulations on the 30–50 day time scale. *J. Atmos. Sci.*, **42,** 364–375.

Kuo, H. L., 1965: On formation and intensification of the tropical cyclones through latent heat release by cumulus convection. *J. Atmos. Sci.*, **22,** 40–63.

——, 1974: Further studies of the parameterization of the effect of cumulus convection on large-scale flow. *J. Atmos. Sci.*, **31,** 1232–1240.

Lau, K.-M., and P. H. Chan, 1983a: Short-term climate variability and atmospheric teleconnections from satellite-observed outgoing longwave radiation. Part I: Simultaneous relationships. *J. Atmos. Sci.*, **40,** 2735–2750.

——, and ——, 1983b: Short-term climate variability and atmospheric teleconnections from satellite-observed outgoing longwave radiation. Part II: Lagged correlations. *J. Atmos. Sci.*, **40,** 2751–2767.

——, and ——, 1985: Aspect of the 40–50 day oscillation during the northern winter as inferred from outgoing longwave radiation. *Mon. Wea. Rev.*, **113,** 1889–1909.

Lau, N.-C., and L. Peng, 1987: Origin of low-frequency (intraseasonal) oscillations in the tropical atmosphere. Part I: Basic theory. *J. Atmos. Sci.*, **44,** 950–972.

——, I. M. Held, and J. D. Neelin, 1988: The Madden–Julian oscillation in an idealized general circulation model. *J. Atmos. Sci.*, **45,** 3810–3832.

Lindzen, R., 1974a: Wave–CISK in the Tropics. *J. Atmos. Sci.*, **31,** 156–179.

——, 1974b: Wave–CISK and tropical spectra. *J. Atmos. Sci.*, **31,** 1447–1449.

Lord, S. J., 1982: Interaction of a cumulus ensemble with the large-scale environment. Part III: Semi-prognostic test of the Arakawa–Schubert cumulus parameterization. *J. Atmos. Sci.*, **39,** 88–103.

——, and A. Arakawa, 1980: Interaction of a cumulus ensemble with the large-scale environment. Part II. *J. Atmos. Sci.*, **37,** 2677–2692.

Madden, R. A., and P. R. Julian, 1971: Detection of a 40–50 day oscillation in the zonal wind in the tropical Pacific. *J. Atmos. Sci.*, **28,** 702–708.

——, and ——, 1972: Description of global-scale circulation cells in the tropics with a 40–50 day period. *J. Atmos. Sci.*, **29,** 1109–1123.

Manabe, S., J. S. Smagorinsky, and R. F. Strickler, 1965: Simulated climatology of a general circulation model with a hydrological cycle. *Mon. Wea. Rev.*, **93,** 769–798.

Neelin, J. D., and I. M. Held, 1987: Modeling tropical convergence based on the moist static energy budget. *Mon. Wea. Rev.*, **115,** 3–12.

——, I. M. Held, and K. H. Cook, 1987: Evaporation–wind feedback and low-frequency variability in the tropical atmosphere. *J. Atmos. Sci.*, **44,** 2341–2348.

Nehrkorn, T., 1986: Wave–CISK in a baroclinic basic state. *J. Atmos. Sci.*, **43,** 2773–2791.

Numaguti, A., and Y. Y. Hayashi, 1991a: Behaviors of the cumulus activity and the structures of the circulations in the 'aqua planet' model. Part I: The structure of the super clusters. *J. Meteor. Soc. Japan,* **69,** 541–561.

——, and ——, 1991b: Behaviors of the cumulus activity and the structures of the circulations in the 'aqua planet' model. Part II: Large scale structures and the evaporation–wind feedback. *J. Meteor. Soc. Japan,* **69,** 563–579.

Ooyama, K., 1964: A dynamical model for the study of tropical cyclone development. *Geofis. Int.* (Mexico), **4,** 187–198.

Randall, D. A., and J. Wang, 1992: The moist available energy of a conditionally unstable atmosphere. *J. Atmos. Sci.*, **49,** 240–255.

Stark, T. E., 1976: Wave–CISK and cumulus parameterization. *J. Atmos. Sci.*, **33,** 2383–2391.

Stevens, D. E., and R. Lindzen, 1978: Tropical wave–CISK with a moisture budget and cumulus friction. *J. Atmos. Sci.*, **35,** 940–961.

Sui, C.-H., and K.-M. Lau, 1989: Origin of low-frequency (intraseasonal) oscillations in the tropical atmosphere. Part II: Structure and propagation of mobile wave–CISK modes and their modification by lower boundary forcings. *J. Atmos. Sci.*, **46,** 37–56.

Xu, K.-M., and K. A. Emanuel, 1989: Is the tropical atmosphere conditionally unstable? *Mon. Wea. Rev.*, **117,** 1471–1479.

Yamasaki, M., 1969: Large-scale disturbances in a conditionally unstable atmosphere in low latitudes. *Papers Meteor. Geophys.*, **20,** 289–336.

Yanai, M., S. Esbensen, and J.-H. Chu, 1973: Determination of bulk properties of tropical cloud clusters from large-scale heat and moisture budgets. *J. Atmos. Sci.*, **30,** 611–627.

Yano, J., and K. A. Emanuel, 1991: An improved model of the equatorial troposphere and its coupling with the stratosphere. *J. Atmos. Sci.*, **48,** 377–389.